Vol. 143: 271–282, 1996 | MARINE ECOLOGY PROGRESS SERIES Mar Ecol Prog Ser | Published November 14

Trends in inorganic and organic carbon in a bloom of *Emiliania huxleyi* in the North Sea

Erik Buitenhuis*, Judith van Bleijswijk, Dorothee Bakker, Marcel Veldhuis

Netherlands Institute for Sea Research, PO Box 59, 1790 AB Texel, The Netherlands

ABSTRACT: During a survey of the end phase of an *Emiliania huxleyi* bloom in the northern part of the North Sea we measured total inorganic carbon (TIC) and the fugacity of CO_2 (fCO_2), as well as standing stocks of $CaCO_3$ and particulate organic carbon (POC). Production of $CaCO_3$ by *E. huxleyi* resulted in an immediate increase of fCO_2, but led to a long-term decrease in fCO_2. Observations during a surface survey and at 24 h stations showed a large increase of fCO_2 with the standing stock of $CaCO_3$. The immediate increase of fCO_2 is caused by a shift in the chemical equilibria in the inorganic carbon system when alkalinity decreases relative to dissolved inorganic carbon (DIC). Average fCO_2 in the high reflectance area (with high numbers of detached coccoliths) was lower than average fCO_2 in the reference areas, located outside the *E. huxleyi* bloom. The long-term decrease in fCO_2 is due to an enhanced sedimentation of both organic and inorganic carbon in faecal pellets containing heavy calcite. This enhanced sedimentation is reflected in the vertical gradient of TIC between the surface mixed layer and the aphotic zone, which increased from the POC-rich zone to the $CaCO_3$ maximum. The overall effect of production, air-sea exchange, mineralisation and sedimentation was a decrease of fCO_2 due to a net transport of carbon to below the pycnocline. We tentatively calculate an atmospheric carbon sink of 1.3 mol m^{-2} for this bloom of *E. huxleyi*.

KEY WORDS: TIC · fCO_2 · $CaCO_3$ · POC · Algal bloom · Coccolithophorid

INTRODUCTION

Emiliania huxleyi (Lohmann) Hay & Mohler is a coccolithophorid of the class of Prymnesiophyta. It is a unicellular alga that produces organic carbon through photosynthesis and inorganic carbon through coccolithogenesis. The coccoliths of *E. huxleyi* are oval platelets which are formed intracellularly by precipitation of $CaCO_3$ in a coccolith vesicle (Westbroek et al. 1989). After completion they are transported out of the cell and retained on the cell surface.

Massive blooms of this species are a regular (yearly) phenomenon, especially in the temperate regions. Surface waters with spectral signatures similar to that of *Emiliania huxleyi* blooms annually covered an average of 1.4×10^6 km^2 (Brown & Yoder 1994). *E. huxleyi* may influence global climate with 3 mechanisms: (1) by affecting the inorganic carbon system of the sea water; (2) by altering the heat exchange between the sea water and the atmosphere, due to increased light scattering by detached coccoliths; and (3) by contributing to emissions of dimethylsulphide (DMS), which increases cloud albedo. In this paper we focus mainly on the first mechanism and to some extent on the second.

All algae contain the enzyme ribulose bisphosphate carboxylase oxygenase (Rubisco). Rubisco fixes CO_2 into organic carbon (Eq. 1), which decreases the CO_2 concentration in the sea water. Besides organic carbon, *Emiliania huxleyi* also produces $CaCO_3$ (Eq. 2). Production of $CaCO_3$ generates CO_2 intracellularly (Eq. 3). The ratio between the production of organic carbon and $CaCO_3$ determines the net effect on the CO_2 concentration in the sea water. Production of organic carbon and $CaCO_3$ in a ratio of 1:1 (Eq. 4) results in a small decrease of the CO_2 concentration. This decrease is caused by the buffering effect of sea water: removal of bicarbonate is partially compensated for by hydration of CO_2. The concentration of CO_2 remains constant if the ratio is 1:1.2. Higher ratios result in elevated CO_2 concentrations.

*E-mail: bhuis@nioz.nl

$$CO_2 + H_2O \rightarrow (CH_2O)_{organic} + O_2 \quad (1)$$

$$HCO_3^- + Ca^{2+} \rightarrow CaCO_3 + H^+ \quad (2)$$

$$HCO_3^- + H^+ \rightarrow CO_2 + H_2O \quad (3)$$

$$2\,HCO_3^- + Ca^{2+} \rightarrow (CH_2O)_{organic} + CaCO_3 + O_2 \quad (4)$$

Laboratory experiments have shown that the ratio between organic carbon and $CaCO_3$ production is affected by the growth conditions of *Emiliania huxleyi*. $CaCO_3$ production has been observed to exceed photosynthesis when cells are limited by phosphate (Paasche & Brubak 1994, van Bleijswijk et al. 1994b). Such a situation may occur at the end of a bloom.

In the field the situation is complicated by the variability of environmental factors. Furthermore sedimentation may play an important role in the field, whereas it cannot be measured in the laboratory. Therefore no *a priori* conclusions can be drawn with respect to the effect of *Emiliania huxleyi* blooms on the CO_2 concentration of surface waters. In order to resolve this question we measured the concentrations and standing stocks of carbon (fCO_2, TIC, $CaCO_3$, POC) in various stages of a bloom of *E. huxleyi* in the summer of 1993 in the North Sea. We derive a carbon budget for the development of the bloom (in time) based on the various stages of the bloom encountered on a transect from the edge to the centre of the bloom (in space).

The fugacity of CO_2 (fCO_2) is proportional to the chemical activity (μ) of CO_2 in air (equivalent to the activity of a dissolved ion). fCO_2 is about 0.5% lower than the partial pressure of CO_2 (pCO_2, equivalent to the concentration of a dissolved ion). Total inorganic carbon (TIC) is the sum of dissolved inorganic carbon (DIC) and $CaCO_3$. Calcium carbonate ($CaCO_3$) is precipitated by *Emiliania huxleyi* into coccoliths in the mineral form calcite (Young et al. 1991). Particulate organic carbon (POC) here designates the organic carbon in algae, calculated from flow cytometer data. Alkalinity is the excess of strong cations over strong anions or the amount of acid needed to titrate weak bases to their protonated forms. Alkalinity was calculated from DIC and fCO_2.

MATERIALS AND METHODS

During a cruise in the northern part of the North Sea (Fig. 1A) from 28 June until 12 July 1993 total inorganic carbon (TIC), fCO_2, standing stocks of $CaCO_3$ and particulate organic carbon (POC) (see Table 1) were measured on board the research vessel 'Pelagia' For TIC, fCO_2, and $CaCO_3$, both discrete samples at CTD stations and on-line measurements, when the ship was sailing, were taken. For POC only discrete samples were taken.

Sampling. Discrete samples were taken from a CTD rosette sampler (Neil Brown) equipped with 10.5 l NOEX bottles. Samples were not poisoned; they were stored in the dark and analysed shortly after sampling. Discrete samples for TIC were taken in gas tight bags made of Mailar (aluminium foil coated with plastic) fitted with gas tight tubing (Masterflex 6542-24). TIC was measured within 2 h after sampling. Discrete samples for fCO_2 were taken in 1100 ml bottles of dark glass, which were flushed with 3 volumes of sea water. The fCO_2 was measured within 1 h after sampling.

On-line samples for TIC were taken at approximately 10 min intervals from a 10 l debubbling tank. This tank was flushed with water from the aqua flow system (flow approximately 8 l min^{-1}) which took in water at a depth of approximately 3 m at the bow of the ship. On-line samples for fCO_2 were taken directly from the aqua flow system. Water temperature, salinity, fluorescence and atmospheric pressure were logged automatically at 1 min intervals.

Total inorganic carbon. Total inorganic carbon (TIC) was measured with an automated coulometer (DOE). Measurements were calibrated with standard water obtained from A. G. Dickson (Scripps Institution of Oceanography, CA, USA). The extraction efficiency as determined with this standard water was 99.3%. The standard deviation was 8 µmol kg^{-1} (n = 19). This relatively large standard deviation was probably caused by variation between titration cells (A. A. J. Majoor, Netherlands Institute for Sea Research, NIOZ, The Netherlands, pers. comm.), which were not calibrated separately. All measurements at a station were performed with the same cell, probably leading to less variation.

Fugacity of CO_2. The mole fraction of CO_2 (xCO_2) in air equilibrated with sea water was measured with an IRGA (infra-red gas analyser, Licor 6252). The instrument resembles the underway system described by Wanninkhof & Thoning (1993), with 3 improvements (design by M. H. C. Stoll and J. M. J. Hoppema, NIOZ). (1) The xCO_2 is measured in non-flowing gas to guarantee that measurements are taken at atmospheric pressure and to obtain a stable signal. Typical standard deviation of 10 measurements was 0.05 ppm. (2) During equilibration the gas is circulated through both the sample cell and the equilibrator. This prevents the flow of unequilibrated air into the system which Wanninkhof & Thoning (1993) mentioned as a possible source of error. (3) Measurements were performed in dry gas to circumvent the need for water vapour correction, and to facilitate comparison between samples and calibration gases.

The IRGA was calibrated every hour with 3 mixtures of CO_2 in synthetic air. The raw data were fitted by a second order function. The polynomial function sup-

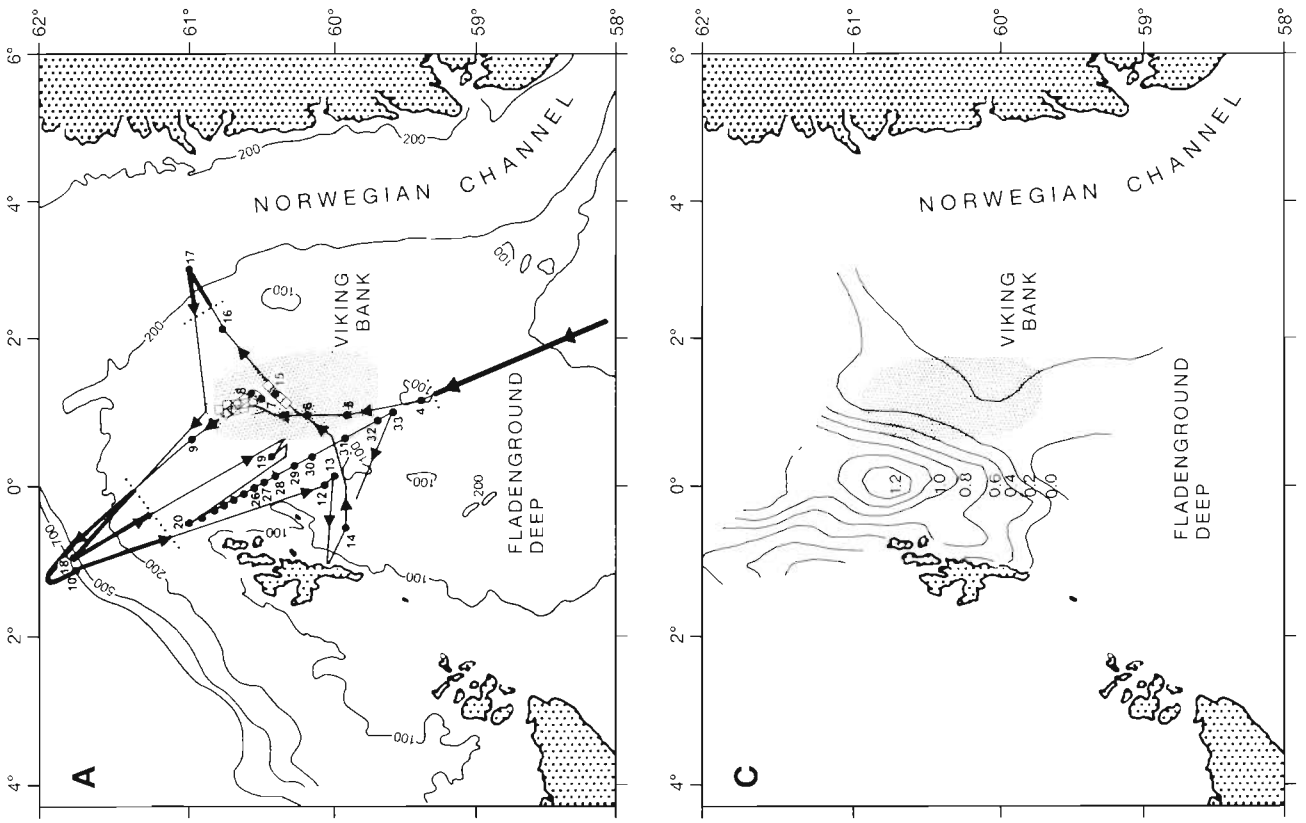

Fig. 1. The research area. (A) Cruise track (from 28 June until 12 July) with station numbers. Stns 19N and 19S are represented by a single dot. Stns 20 to 33 are referred to as the transect. Shaded area indicates the average position of the high reflectance area between 27 June and 13 July. (□) On-line data in the high reflectance area. Bold lines: on-line data in the reference areas. (B) AVHRR photograph of the investigated area on 27 June 1993. The high reflectance area can be recognised as a light spot between The Shetlands and Norway. Dark spots are cloud cover (C) Contour plot of the fluorescence (arbitrary units) at 3 m depth in the investigated area

plied by the manufacturer gives less reproducible results for xCO_2, because the zero and span settings vary with changes in pressure and temperature (F. A. Koning, NIOZ, pers. comm.).

The 3 calibration gases were calibrated on a gas chromatograph (GC) against 3 standards of the NMI (Dutch Bureau of Standards). Similarly, a calibration gas of NOAA (National Oceanographic and Atmospheric Administration, USA) was measured on the GC. The difference between the measured value based on the NMI calibration and the value given by NOAA was +1.3 ppm. The reproducibility of the IRGA, calculated as the standard deviation of air samples (n = 133), was 1.2 ppm.

Discrete samples for xCO_2 were measured in bottles of dark glass after equilibration of 1 l sea water with 100 ml laboratory air plus the volume of air in the instrument. On-line samples were taken by equilibrating a circulated flow of air with a continuous flow of sea water from the aqua flow system (approximately 2 l min^{-1}) in an equilibrator equipped with a calibrated temperature sensor. The design of the equilibrator was adopted from A. Watson (Robertson et al. 1993). Every hour we measured 10 samples from the sea water equilibrator and 1 sample of air, taken at about 15 m above the sea surface.

For the discrete samples, fCO_2 was calculated using xCO_2, the temperature measured by the CTD and the ambient pressure (Weiss 1974). This calculated fCO_2 was higher than the *in situ* fCO_2 due to warming of the samples. We estimate an increase of less than 10 µatm for surface samples and less than 60 µatm for samples taken at 125 m.

For the on-line samples, fCO_2 in the equilibrator was calculated using the temperature in the equilibrator and the ambient pressure. fCO_2 at the *in situ* temperature was calculated from TIC and alkalinity according to Goyet et al. (1993). The use of TIC instead of DIC introduced an error smaller than 0.1 µatm. TIC at the time of measurement of fCO_2 was obtained by linear interpolation. Alkalinity was calculated using TIC and fCO_2 in the equilibrator.

Dissolved inorganic carbon and alkalinity. Dissolved inorganic carbon (DIC) was calculated by subtracting $CaCO_3$ from TIC. Alkalinity was calculated from DIC and fCO_2, using the dissociation constants of Goyet & Poisson (1989). The uncertainty in alkalinity due to the standard deviation of 8 µmol kg^{-1} in TIC is about 10 µequivalents kg^{-1}. The uncertainty due to the standard deviation of 1.2 ppm in fCO_2 is about 1 µequivalent kg^{-1}.

Standing stock of $CaCO_3$. Particulate calcium (>0.8 µm) standing stock was determined according to van Bleijswijk et al. (1994a) using atomic absorption spectroscopy. The reproducibility of the measurements (average standard deviation of duplicates) was 6%. The $CaCO_3$ standing stock was calculated from particulate calcium by assuming a 1:1 Ca:C molar ratio in coccoliths (K. M. Fagerbakke, University of Bergen, Norway, pers. comm.).

Dissolution of $CaCO_3$. The dissolution rate of $CaCO_3$ was determined by incubating 5 l of sea water in the dark. Duplicate samples were taken in the dark from single 10.5 l NOEX bottles. Samples were incubated unfiltered or after filtration over 10 and 200 µm filters to remove micro- and mesozooplankton respectively. Samples were incubated in a sea water tank on deck of the ship. Subsamples were taken after 0, 24 and 48 or 72 h, until the bottles were empty. Three series of subsamples in which a decrease in $CaCO_3$ alternated with an increase were discarded. Apparently the bottles had not been shaken sufficiently to resuspend the coccoliths and algae before taking one of the subsamples.

Saturation of sea water with $CaCO_3$. The concentration of calcium ($[Ca^{2+}]$) was measured by atomic absorption spectroscopy. The concentration of carbonate ($[CO_3^{2-}]$) was calculated from DIC and fCO_2, using the dissociation constants of Goyet & Poisson (1989). The extent of oversaturation of $CaCO_3$ in sea water was calculated according to Mucci (1983).

Particulate organic carbon. Particulate organic carbon (POC) standing stock of the phytoplankton was calculated from cell numbers and estimated spherical diameters (ESDs), as determined by flow cytometry (Veldhuis et al. in press). ESD was calibrated with standard beads (high density 2.0 and 10.0 µm, Coulter Counter), and checked by fractionated filtration and microscopical observations. ESDs were used to estimate cell volumes (assuming spherical cells), that were converted to carbon. For cyanobacteria a constant factor of 400 fg C $µm^{-3}$ was used (Takahashi et al. 1985). For pico-eukaryotes a factor of 1800 to 3000 fg $cell^{-1}$ was used, depending on size (Campbell & Vaulot 1993). For larger cells the formula $\log C = -0.422 + 0.758 \log V$ was used (Strathmann 1967). Detritus was not included.

RESULTS

Research area

Before the start of the cruise the research area was located by AVHRR (advanced very high resolution radiometry). An area with high reflectance was observed in the North Sea. During the cruise this area was located east of the Shetland Islands (Fig. 1B). The high reflectance area could be recognised from the ship as a milky white colouring of the sea. It was characterised by low nutrient concentrations (NO_3^- and

PO_4^{3-} < 0.1 µmol l^{-1}), low particulate organic carbon (~4 µmol l^{-1} POC), low numbers of living *Emiliania huxleyi* (~2000 ml^{-1}) and high numbers of detached coccoliths (~100 000 ml^{-1}). These conditions are typical for the end phase of a bloom of *E. huxleyi*. Small cyanobacteria (~100 000 ml^{-1}) contributed about 50% to POC.

To the northwest of the high reflectance area we observed a POC-rich zone (cf. Fig. 1C). This zone was characterised by high nutrient concentrations (4 µmol l^{-1} NO_3^-, 0.3 µmol l^{-1} PO_4^{3-}) and a high standing stock of POC (~30 µmol l^{-1}). A mixed phytoplankton community was present, with *Emiliania huxleyi* (~3500 ml^{-1}) constituting about 40% of POC.

In the Atlantic Ocean and to the east and south of the high reflectance area nutrient concentrations (0.1 to 6 µmol l^{-1} NO_3^- and 0.1 to 0.4 µmol l^{-1} PO_4^{3-}) and POC (2 to 15 µmol l^{-1}) were variable. In these areas, which we will call the reference areas (Fig. 1A), the numbers of *Emiliania huxleyi* cells (~2000 ml^{-1}) and detached coccoliths (~16 000 ml^{-1}) were low.

On-line measurements

Total inorganic carbon (TIC; Table 1) averaged 2048 ± 31 µmol kg^{-1} (n = 172) in the high reflectance area, and 2058 ± 31 µmol kg^{-1} (n = 182) in the reference areas. TIC varied between 1970 and 2110 µmol kg^{-1} in both areas. fCO_2 in the high reflectance area was 303 ± 24 µatm on average (n = 464, ranging from 257 to 440 µatm). In the reference areas fCO_2 was 324 ± 29 µatm on average (n = 416, ranging from 227 to 421 µatm).

Apparently, the 2 regions, while showing large differences in detached coccoliths, do not show significant differences in average TIC and fCO_2. However, we found a positive correlation between fCO_2 and on-line $CaCO_3$ standing stock measured at the same time [fCO_2 (µatm) = 259.7 + 3.5 $CaCO_3$ (µmol l^{-1}), n = 94, p < 0.05]. When fCO_2 was corrected to a constant temperature of 10.6°C it increased slightly less with $CaCO_3$ [Fig. 2; fCO_2-corrected (µatm) = 260.0 + 3.0 $CaCO_3$ (µmol l^{-1}), n = 94, p < 0.05]. We also observed a positive correlation between temperature and $CaCO_3$ standing stock [T (°C) = 10.6 + 0.03 $CaCO_3$ (µmol l^{-1}), n = 94, p < 0.02]. Ackleson et al. (1988) and Holligan et al. (1993) found a much larger temperature difference between $CaCO_3$-rich and $CaCO_3$-poor waters.

The mole fraction of CO_2 (xCO_2) in dry air was 358.8 ± 1.2 ppm (n = 133) during the first week of the cruise. The same average xCO_2 was presented in Boden et al. (1994) for June 1993 north of 35° N (357.6 ± 3.7, n = 8, excluding the data of the industry-influenced Waldhof station). fCO_2 in the air, at a pressure of 1.013×10^5 Pa and an average *water* temperature of 11.6°C, was 357.5 µatm.

24 h stations

At four 24 h stations (Stns 12, 19N, 19S and 15; Fig. 1A) we measured several vertical profiles of TIC, fCO_2, $CaCO_3$ and POC over a 24 h period. The position of the ship was maintained in relation to the sam-

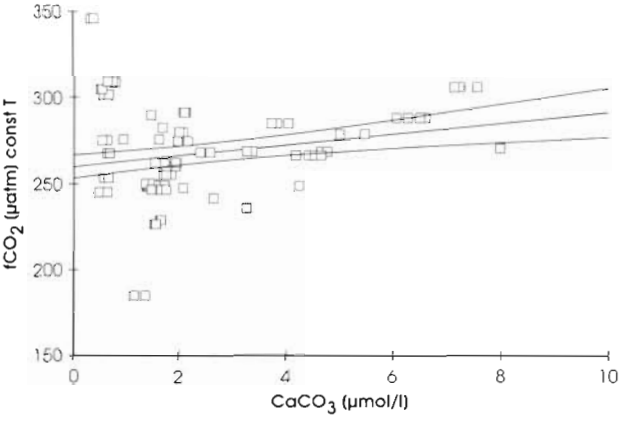

Fig. 2. Plot of fugacity of CO_2 (fCO_2), corrected to a constant temperature of 10.6°C, versus $CaCO_3$. Linear regression with 95% confidence levels, fCO_2 = 260.0 + 3.0 $CaCO_3$, n = 94, p < 0.05

Table 1. Parameters mentioned in this paper

Parameter	Abbreviation	Unit	Description
Alkalinity		µequivalents kg^{-1}	$2[CO_3^{2-}] + [HCO_3^-] + [B(OH)_4^-] + [OH^-] - [H^+]$ etc.
Calcite	$CaCO_3$	µmol l^{-1}	Particulate Ca (>0.8 µm)
Chlorophyll *a*		µg l^{-1}	Measured fluometrically or with HPLC
Dissolved inorganic carbon	DIC	µmol kg^{-1}	$[HCO_3^-] + [CO_3^{--}] + [CO_2]$
Fugacity of CO_2	fCO_2	µatm	Activity of CO_2 gas in water
Mole fraction of CO_2	xCO_2	ppm	Gas mixing ratio (µmol mol^{-1})
Particulate organic carbon	POC	µmol l^{-1}	Phytoplankton carbon (flow cytometer)
Total inorganic carbon	TIC	µmol kg^{-1}	$[HCO_3^-] + [CO_3^{--}] + [CO_2] + [CaCO_3]$

pled water mass by using a drifting buoy with sediment traps at 10 and 50 m depth. Stn 12 was located just outside the high reflectance area. To the west of the high reflectance area there were two 24 h stations on the same day (sampled alternatingly). One (Stn 19N) was located in the POC-rich zone, and the other (Stn 19S) was located 9 nautical miles to the south, towards the high reflectance area. The fourth 24 h station (Stn 15) was in the high reflectance area.

At none of the stations did fCO_2 or TIC show a distinct diel rhythm. In order to better distinguish the differences between stations, data of all CTD casts were averaged to produce a single profile per station. We order these stations as progressive stages of the bloom: first the reference areas, then the POC-rich zone and then the high reflectance area (successively Stns 12, 19N, 19S and 15). During these stages concentrations of TIC decreased in the upper mixed layer (from 2070 to 2060 µmol kg^{-1}). In contrast, below the pycnocline TIC increased (from 2120 to 2150 µmol kg^{-1}) (Fig. 3A). These observations indicate that sedimentation was higher in the high reflectance area than in the reference areas. Sedimentation decreases TIC in the upper mixed layer, and subsequent mineralisation below the pycnocline increases TIC. The fCO_2 increased from Stn 12 to Stn 15 over the entire water column (from 286 to 354 µatm at the surface, Fig. 3B). Stns 19S and 19N showed intermediate values.

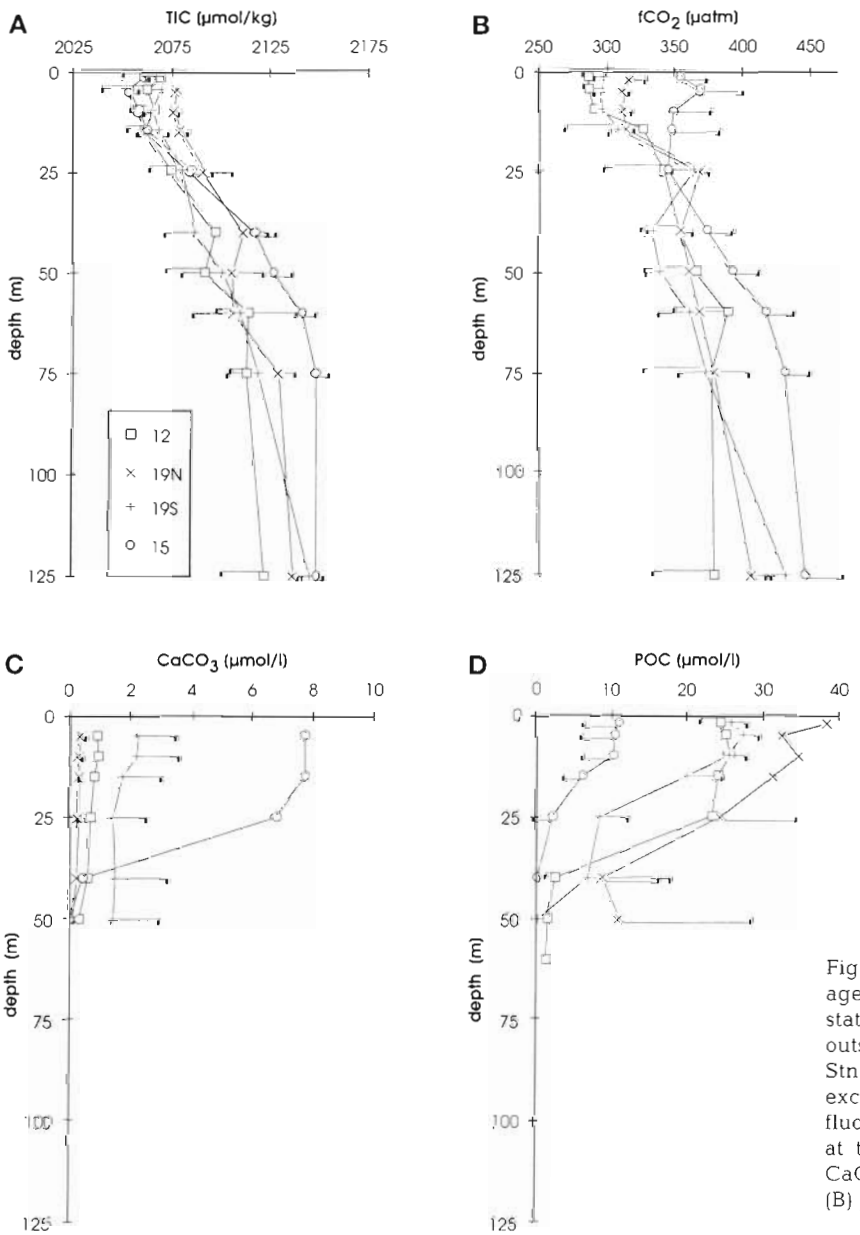

Fig. 3. Depth profiles of 24 h stations, averaged values over all CTD casts at a single station, with standard deviations. (□) Stn 12, outside the bloom (n = 3, except $CaCO_3$); (×) Stn 19N, at the fluorescence maximum (n = 3, except $CaCO_3$); (+) Stn 19S, at the lower fluorescence (n = 4, except $CaCO_3$); (○) Stn 15, at the high reflectance area (n = 5, except $CaCO_3$). (A) Total inorganic carbon, TIC; (B) fCO_2; (C) $CaCO_3$; (D) POC (n = 1 or 2 for Stns 19N, 19S)

The standing stock of $CaCO_3$ increased from Stn 19N via 19S to Stn 15, whereas the standing stock of POC decreased (Fig 3C, D). At Stn 12 the standing stocks of $CaCO_3$ and POC were intermediate between those at Stns 19N and 19S.

At Stn 15 a high standing stock of $CaCO_3$ (8 µmol l^{-1}) and a low standing stock of POC (11 µmol l^{-1}) coincided with a high fCO_2 (354 µatm at the surface). Most likely, this high fCO_2 is the result of the acidification of the sea water due to $CaCO_3$ production (Eqs. 2 & 3). At another station in the high reflectance area (Stn 7, Fig. 1A) a high $CaCO_3$ standing stock (15 µmol l^{-1}) and low POC (4 µmol l^{-1} at the surface) coincided with a low fCO_2 (330 µatm at the surface, data not shown). The vertical gradient in TIC (2040 µmol kg^{-1} at the surface; 2150 µmol kg^{-1} at 125 m depth) was even sharper here than at Stn 15. We conclude that so much carbon was removed from the upper mixed layer through sedimentation that this had a greater effect on fCO_2 than did the production of coccoliths.

Dissolution experiments

At Stns 7, 12 and 15 (Fig. 1A) samples were incubated in the dark for determination of the dissolution rate of $CaCO_3$. In order to determine the effect of grazing on the dissolution rate we compared samples that had been filtered before incubation (either 10 or 200 µm) with unfiltered samples. Removal of grazers had no significant effect on the dissolution rate of $CaCO_3$ (data not shown). Therefore the results were averaged per station (Fig. 4). At all stations 25% (±11%, n = 27) of the $CaCO_3$ standing stock dissolved per 24 h.

The sea water at Stns 7, 12 and 15 was 3.8 to 4.5 times oversaturated with respect to $CaCO_3$. Even if all the POC in the samples had been mineralised to CO_2 during the incubations the sea water would still be oversaturated 3.6 to 4.1 times with respect to $CaCO_3$.

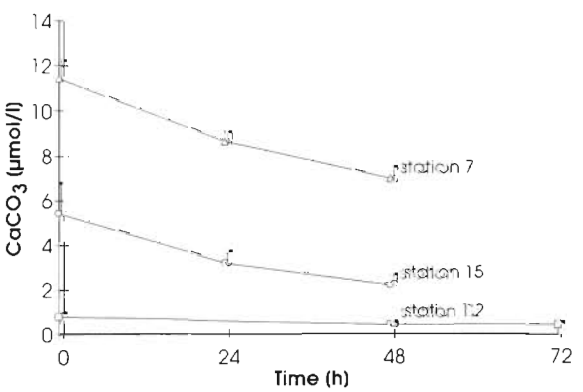

Fig. 4. Changes in standing stocks of $CaCO_3$ of samples stored in the dark, with standard deviations. (□) Stn 12, (○) Stn 15, (△) Stn 7

Transect

Within a period of 24 h vertical profiles were taken along a transect (Stns 20 to 33; Fig. 1A). This transect ran from the edge of the Atlantic Ocean, through the POC-rich zone, along the edge of the high reflectance area where coccoliths were abundant.

TIC and the density of the water (SigmaT) showed comparable patterns (Fig. 5A, B). Towards the high reflectance area the gradients of TIC and SigmaT with depth became more pronounced. An increased gradient of TIC with depth was noted above (in the section '24 h stations'), and indicates increased sedimentation. The fCO_2 was clearly influenced by uptake of CO_2 by algae, expressed as POC (Fig. 5C, D). A minimum of fCO_2 was located in the POC-rich zone. Low values of fCO_2 persisted in the high reflectance area. There was no apparent relationship between $CaCO_3$ and fCO_2 (Fig. 5D, E). Calculated alkalinity in the upper mixed layer decreased from the POC-rich zone to the high reflectance area. This agrees with the observed increase of the standing stock of $CaCO_3$ (Fig. 5E, F).

The $CaCO_3$ standing stock, as measured by atomic absorption, showed a close correlation with the $CaCO_3$ standing stock calculated from flow cytometer data ($CaCO_3^{AAS} = 0.99\,CaCO_3^{flow\ cytometer} - 0.052$, $p < 0.001$, n = 39). For Stns 20, 22, 30 and 32 we assumed that each *Emiliania huxleyi* cell was covered with 20 coccoliths. The total number of coccoliths (attached and detached) was multiplied by 0.26 pg C $coccolith^{-1}$ (Balch et al. 1992). At Stns 24, 26 and 28 (the POC-rich zone) $CaCO_3$ was calculated from detached coccoliths only, because the numbers of *E. huxleyi* cells were probably overestimated due to the presence of small diatoms (P. van der Wal, NIOZ, pers. comm.). At Stn 33 (95 nautical miles from the start of the transect) $CaCO_3$ was not measured by atomic absorption spectrophotometry (AAS), but estimated using this equation.

The organic carbon to chlorophyll ratio [POC (µmol l^{-1})/chlorophyll *a* (µg l^{-1})] was 6.7 ± 3.8 (n = 43) on average. In the POC-rich zone the ratio was 9 ± 5 (n = 17). In the high reflectance area it was 4 ± 2 (n = 15). Because organic carbon was calculated from flow cytometer data for living algae, the ratio is a direct measure of the average algal composition.

Total carbon content (TIC + POC; Fig. 6) was calculated over the photic zone (0 to 40 m, penetration depth of 0.5% of surface irradiance) and the aphotic zone (40 to 80 m), and over the entire sampled depth (0 to 80 m). Proceeding from the POC-rich zone towards the high reflectance area the total carbon content decreased in

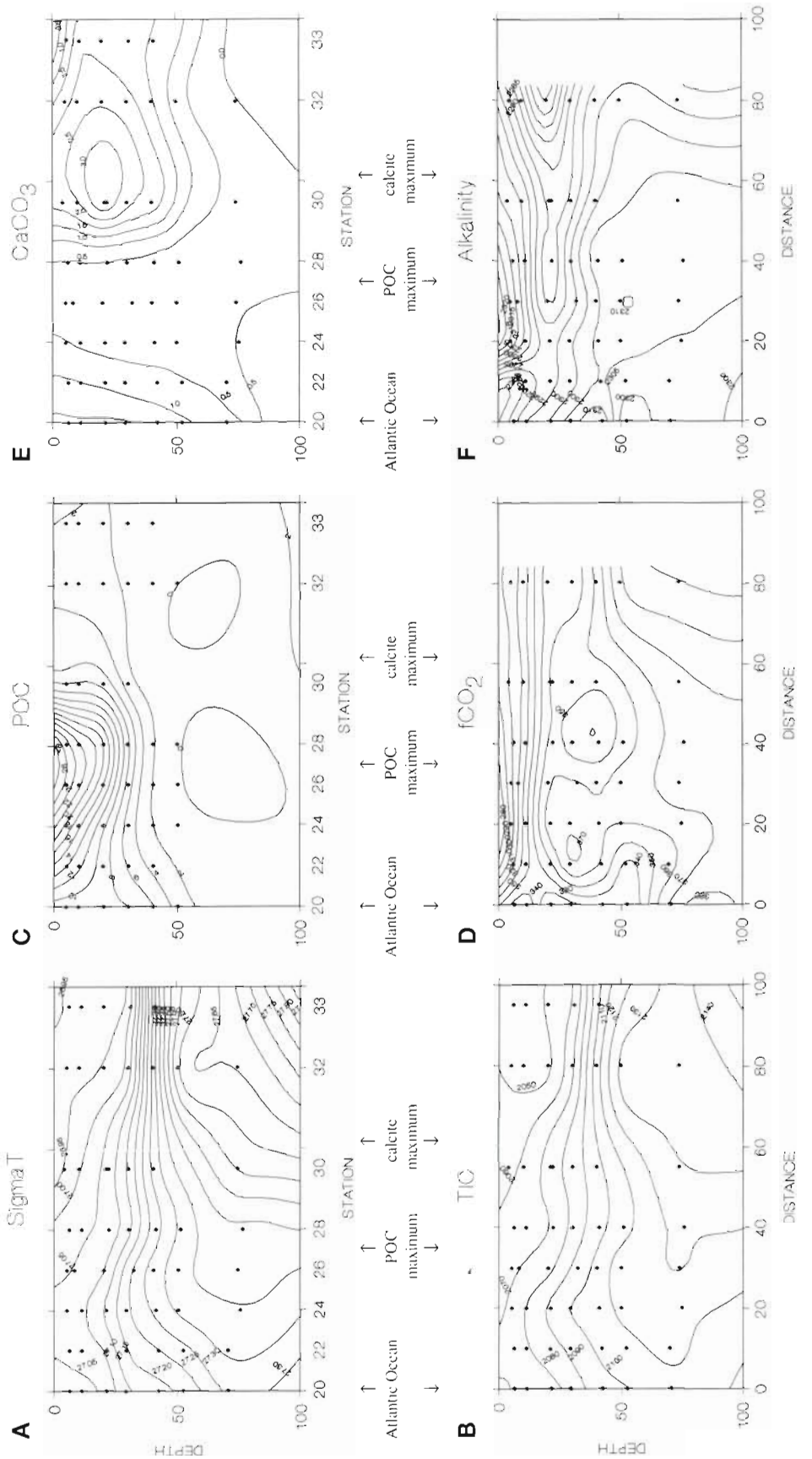

Fig. 5. Contour plots (using least squares method) of the transect, with distance from the first station in nautical miles and depth in meters. Diamonds represent sampling depths. fCO_2 and $CaCO_3$ were not measured at the last station. (A) SigmaT is the density excess calculated as [density (kg l^{-1}) −1] × 1000. (B) TIC in µmol kg^{-1} (C) POC in µmol l^{-1} (D) fCO_2 in µatm. (E) $CaCO_3$ in µmol l^{-1} at 95 nautical miles was calculated from flow cytometer data using the correlation of flow cytometer data with atomic adsorption measurements at the other stations (see text). (F) Calculated alkalinity in µequivalents kg^{-1}

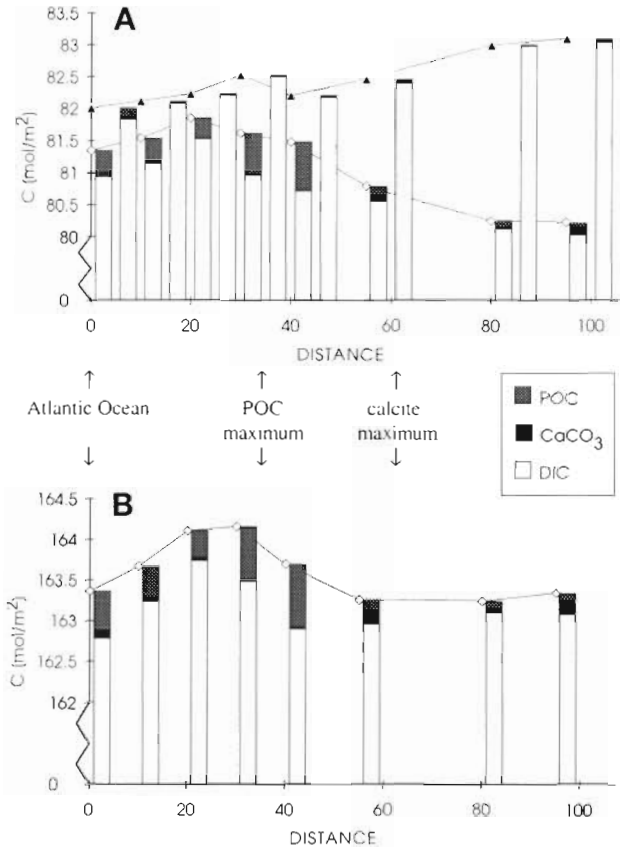

Fig. 6. Total carbon content (ΣC: the sum of TIC and POC) of the water column along the transect, with distance from the first station in nautical miles. Open bars: DIC. Filled bars: $CaCO_3$. Shaded bars: POC. (A) ◇ (odd bars) ΣC in the photic zone: 0 to 40 m depth. ▲ (even bars) ΣC in the aphotic zone: 40 to 80 m depth. (B) ΣC in the sampled water layer: 0 to 80 m depth

the photic zone, whereas it increased in the aphotic zone (Fig. 6A). We ascribe these trends to the sinking of $CaCO_3$ and POC through the stratified layer, and the subsequent dissolution of $CaCO_3$ and degradation of POC below 40 m. Van der Wal et al. (1995) found enhanced sedimentation of both $CaCO_3$ and POC in the high reflectance area due to the increased density of faecal pellets that contained coccoliths.

Total carbon content measured over the entire sampled depth was highest in the POC-rich zone (Fig. 6B). Algal growth and the resultant minimum in fCO_2 has probably led to a high atmosphere-ocean flux of carbon dioxide into this area. In the high reflectance area the total amount of $CaCO_3$ exceeded the total amount of POC (Fig. 6B).

Dissolved organic carbon (DOC) was only measured in the photic zone. DOC was constant at 3.0 ± 0.2 mol m^{-2} (C. P. D. Brussaard, NIOZ, pers. comm., data not shown).

DISCUSSION

In a bloom of *Emiliania huxleyi* in the North Atlantic in 1991 Robertson et al. (1994) found that the fugacity of CO_2 (fCO_2) was 15 µatm higher in waters with high $CaCO_3$ standing stocks (>18 µmol l^{-1}) than in waters with low $CaCO_3$ standing stocks (<5.5 µmol l^{-1}). We will argue here that while the short-term effect of $CaCO_3$ precipitation was a rise in fCO_2 due to a decrease in alkalinity, the long-term effect of this bloom of *E. huxleyi* was a decrease in fCO_2 by enhanced sedimentation. First we discuss the influences that the physical properties of the water column and biological activities have on the concentrations of inorganic and particulate organic carbon and the speciation of the dissolved inorganic carbon system. Then we derive a carbon budget that shows that this bloom acted as a carbon sink for the atmosphere.

The influence of the physical structure was apparent from the similarity between the contour plots for total inorganic carbon (TIC) and the density of the water column (Fig. 6A, B). In the high reflectance area the stratification was more pronounced than in the northern part of the research area (Atlantic Ocean side). As a result the phytoplankton was mixed over shallower depths, and the concentration gradient of inorganic carbon was steeper (Fig. 5B, see also Fig. 6A). The enhancement of stratification is not necessarily the result of physical processes only. *Emiliania huxleyi* may generate a positive feedback for an increase of the temperature in the upper mixed layer: the reflectance of coccoliths may increase the temperature by light scattering (Holligan & Balch 1991, Westbroek et al. 1993), this will make the upper mixed layer shallower which will increase the average light intensity, and this will stimulate growth. The observed positive correlation between temperature and the $CaCO_3$ standing stock illustrates these processes of calcification, stratification and positive feedback.

The influence of biological activities on the carbon speciation was manifested by the occurrence of the fCO_2 minimum in the POC-rich zone, and by the increase of fCO_2 with biologically produced $CaCO_3$. Furthermore TIC was strongly depleted in the upper mixed layer of the high reflectance area, because in this area sedimentation was high due to the elevated sinking speed of faecal pellets containing $CaCO_3$ (van der Wal et al. 1995).

In a plot based on a surface survey over the entire cruise track, fCO_2 (corrected to a constant temperature) increased with an increase of the standing stock of $CaCO_3$ (Fig. 2). This demonstrates that precipitation of $CaCO_3$ shifts the DIC equilibria in favour of CO_2 according to Eqs. (2) and (3). The fCO_2 increased 3.0 µatm per µmol l^{-1} $CaCO_3$. This is much

higher than the increase of fCO_2 that is predicted from $CaCO_3$ precipitation (1 µatm per µmol l^{-1} $CaCO_3$) at typical concentrations of alkalinity and DIC]. The enhanced increase results from the apparent inverse correlation between the standing stocks of POC and $CaCO_3$ (Figs. 3C, D & 5C, E). There are 3 compatible explanations for this inverse correlation. Firstly, the production of $CaCO_3$ continues after the culmination of the bloom, so that the peak in $CaCO_3$ standing stock occurs after the peak in POC standing stock (P. van der Wal pers. comm.). Secondly, other phytoplankton species may contribute relatively less to POC at the end of the bloom, when nutrient concentrations are low. At low nutrient concentrations *Emiliania huxleyi* will outcompete other phytoplankton species as it has a high affinity for nutrients, especially phosphate (Egge 1993). Thirdly, POC is degraded faster than $CaCO_3$, so the relative contribution of $CaCO_3$ increases.

The relatively high fCO_2 in the surface water at Stn 15 (which has a high standing stock of $CaCO_3$) is in accordance with the trend shown in Fig. 2. The profiles of the other 24 h stations do not show a clear increase of fCO_2 with $CaCO_3$. Other data also seem to contradict a positive correlation between $CaCO_3$ and fCO_2. At Stn 7, where the highest standing stock of $CaCO_3$ was found, fCO_2 was relatively low. Along the transect fCO_2 at the surface was fairly constant between Stns 24 and 33. On-line surface measurements of fCO_2 integrated over wider areas were lower inside the high reflectance area than in the reference areas. The explanation is found in the trend in TIC along the transect towards lower concentrations in the upper mixed layer and higher concentrations below the pycnocline. This is consistent with sedimentation, which results in a decrease of fCO_2 at time scales that are slower than the increase of fCO_2 caused by production of $CaCO_3$. We conclude that whether calcification is seen as a sink or source of CO_2 depends on the time scale on which these processes are observed: while on the basis of chemical equilibria production of CaCO3 will lead to an instantaneous increase of fCO_2, the overall processes of production, remineralisation, dissolution, air-sea gas exchange and sedimentation lead to a net export of carbon from the upper mixed layer, and hence a decrease of fCO_2.

About 25% of the standing stock of $CaCO_3$ was found to dissolve per 24 h in the dark, despite the fact that the sea water at Stns 7, 12 and 15 was about 4 times oversaturated with respect to $CaCO_3$. Degradation of the standing stock of POC would not change this. Since there was no significant difference between filtered (either 10 or 200 µm) and unfiltered samples, we conclude that dissolution was not caused by micro- or mesozooplankton. Therefore dissolution was probably caused by respiration of bacteria and algae, and by lysis of cells, which creates an acidified micro-environment around the coccoliths.

Photosynthesis accompanied by production of $CaCO_3$ in a molar ratio of 1:1 amounts to bicarbonate utilisation, and leads to a smaller decrease in fCO_2 than in the case of CO_2 utilisation by photosynthesis alone. In either case there is an additional decrease in fCO_2 due to an increase in pH since uptake NO_3^- by the cell is coupled to OH^- excretion (Brewer & Goldman 1976). This increase of pH is equivalent to an increase of alkalinity (Table 1). The ratio between calcification and photosynthesis (C/P ratio) indicates how uptake of dissolved inorganic carbon will affect fCO_2. When the effect of simultaneous production of CaCO3 and POC is calculated, fCO_2 remains constant at a C/P ratio of 1.2:1. When the effect of PON production is also taken into account the C/P ratio required for maintaining a constant fCO_2 increases to 1.3:1. The highest C/P production ratio that was observed in this bloom was 0.18 (Stn 7, van der Wal et al. 1995). The highest C/P sedimentation ratio was 1.3 (Stn 15, the unpoisoned trap at 50 m depth; van der Wal et al. 1995). Thus no indication for an increase of fCO_2 was observed at any stage of this bloom.

The particulate organic carbon to chlorophyll *a* ratio in the POC-rich zone was about twice the ratio in the high reflectance area. Although the difference is not significant, there is an explanation for this difference. The beam attenuation coefficient c530 was twice as large in the high reflectance area as in the POC-rich zone. This would lead to a higher chlorophyll content per cell as an adaptation to low light conditions.

Consecutive stages of the bloom development were encountered travelling southward along the transect. Therefore we tentatively interpret Fig. 6 as the development of the bloom in time. This interpretation is suggested by the seasonal northwesterly migration of the high reflectance area on satellite images taken before the cruise. This is corroborated by the observed decrease of nutrient concentrations from north to south. We have calculated the transport of carbon during the bloom from changes in the total carbon content (TIC + POC) of the sampled water column along the transect. For this purpose the water column was divided into an upper (0 to 40 m), an intermediate (40 to 80 m) and a deep (80 to 130 m) box (Fig. 7). The thermocline resides at approximately 40 m depth (Fig. 5A), whereas no samples were taken below 80 m depth. The mass balance for the upper box involves an influx of CO_2 from the atmosphere, changes in carbon pools and downflux of biogenic particles:

$$\text{Influx} = \Delta\text{DIC} + \Delta\text{POC} + \Delta CaCO_3 + \text{Downflux} \quad (5)$$

This latter downflux is the source term for a similar balance for the intermediate box, where any residual carbon is assumed to represent an excess sedimentation term into the deep box:

Downflux =
$\Delta DIC + \Delta POC + \Delta CaCO_3$ + Excess sedimentation (6)

In the first 20 nautical miles of the transect from the Atlantic Ocean to the POC-rich zone the fCO_2 decreased to 286 µatm at the surface, while the total carbon content from 0 to 80 m increased by 0.7 mol m^{-2} (Figs. 5D & 6B). This indicates uptake of CO_2 from the atmosphere. The air to sea flux (influx; Fig. 7) was calculated with the exchange coefficient for average wind speeds given by Wanninkhof (1992) using the average wind speed during the cruise and the fCO_2 gradient at the chlorophyll maximum (20 nautical miles from the beginning of the transect). At a fugacity gradient of 72 µatm and an average wind speed during the cruise of 7.7 m s^{-1} it would have taken 64 d for an amount of 0.7 mol m^{-2} to be taken up from the atmosphere. This 64 d period is only an approximation since fCO_2 was only measured once at Stn 24 and the wind speed represents an average in time (13 d) and space. Blooms tend to be visible by AVHRR for shorter periods of typically 15 to 30 d (Westbroek et al. 1993). This would mean that either the air to sea flux has been underestimated or diffusion from below the thermocline plays an important role. We have not included the latter diffusion in our calculations.

In the subsequent stretch (20 to 100 nautical miles) from the POC-rich zone (Stn 24) to the high reflectance area (Stn 33) the stratification increased (Fig. 5A). As discussed above, this led to a decrease of DIC in the photic zone (0 to 40 m; Fig. 6A). This decrease cannot be ascribed to increased photosynthesis since neither POC (Figs. 5C & 6A), nor chlorophyll *a* (data not shown) increased, due to nitrogen limitation. Since the total carbon content in the aphotic zone increased while the total carbon content in the photic zone decreased (Fig. 6A) we assume that these changes are caused by sedimentation.

From the POC-rich zone to the high reflectance area the decrease in total carbon content of 1.6 mol m^{-2} in the upper mixed layer was larger than the increase of 0.9 mol m^{-2} in the intermediate layer (Fig. 6B). Since the upper mixed layer remained undersaturated (Fig. 5D), the difference of 0.7 mol m^{-2} cannot have escaped by sea to air outflux. The most straightforward explanation is that from 80 m to the bottom the total carbon content increased as well, as was found elsewhere at the 24 h stations at 125 m depth (Fig. 3). When the measured total carbon content at 80 m depth was extrapolated to the 80 to 130 m interval an increase of 2.4 mol m^{-2} for the aphotic zone (40 to 130 m) was calculated over the whole transect (downflux + excess sedimentation in Fig. 7). In the photic zone the total carbon content decreased 1.1 mol m^{-2}. This would yield an overall atmospheric carbon sink of 1.3 mol m^{-2} for this bloom of *Emiliania huxleyi*. This is consistent with the relatively high sedimentation rate of 45 mmol m^{-2} d^{-1} that was measured at Stn 7 (van der Wal et al. 1995), if it is multiplied by 30 d.

If we calculate the global significance of this carbon sink of 1.3 mol m^{-2} by multiplying it by the average area of *Emiliania huxleyi* blooms of 1.4×10^6 km^2 (Brown & Yoder 1994) we arrive at 2.2 Mt C yr^{-1} or 0.4‰ of the export production at 100 m depth (Berger et al. 1989).

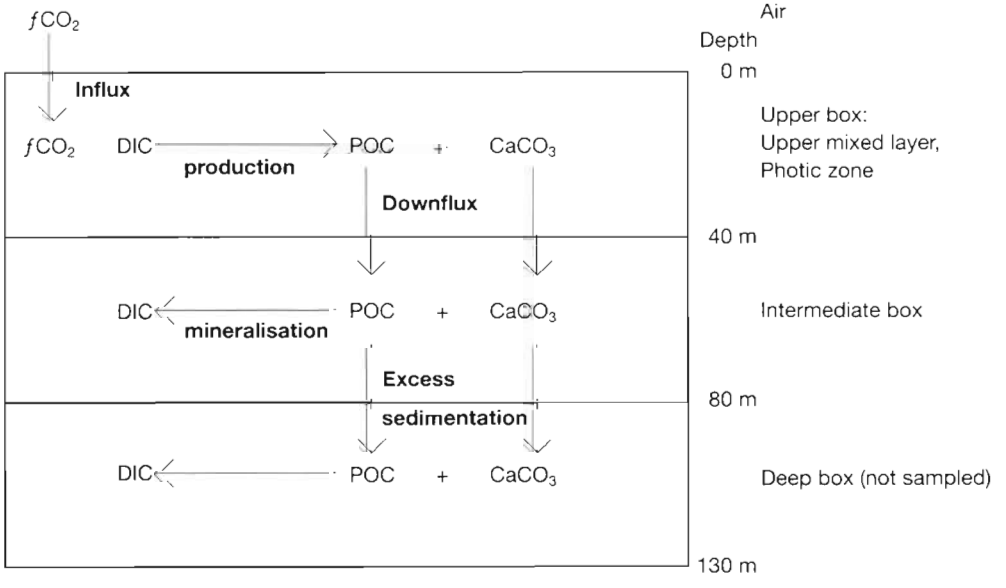

Fig. 7. Box model for a carbon budget. For details see text

Acknowledgements. We thank Rob Kempers, Erica Koning and the captain and the crew of the RV 'Pelagia' for technical assistance. We thank the blood bank in Alkmaar for providing the Mailar. We thank Steve Groom for processing the AVHRR data. Helpful discussions with Erica Koning, Paul van der Wal, Hein de Baar, Dieter Wolff-Gladrow, Ray Weiss, Hein de Wilde and Bram Majoor were appreciated. We thank the reviewers for comments that led to improvement of the manuscript.

LITERATURE CITED

Ackleson S, Balch WM, Holligan PM (1988) White waters of the Gulf of Maine. Oceanography 1(2):18–22

Balch W, Evans R, Brown J, Feldman G, McClain C, Esaias W (1992) The remote sensing of ocean primary productivity: use of a new data compilation to test satellite algorithms. J Geophys Res 97(C2):2279–2293

Berger WH, Smetacek VS, Wefer G (1989) Ocean productivity and paleoproductivity — an overview. In: Berger WH, Smetacek VS, Wefer G (eds) Productivity in the ocean: present and past. John Wiley & Sons Ltd, Chichester, p 1–34

Boden TA, Kaiser DP, Sepanski RJ, Stoss FW (1994) Trends '93: a compendium of data on global change. Carbon dioxide information analysis center, Oak Ridge National Laboratory, Oak Ridge, TN

Brewer PG, Goldman JC (1976) Alkalinity changes generated by phytoplankton growth. Limnol Oceanogr 21(1): 108–117

Brown CW, Yoder JA (1994) Coccolithophorid blooms in the global ocean. J Geophys Res 99(C4):7467–7482

Campbell L, Vaulot D (1993) Photosynthetic picoplankton community structure in the subtropical North Pacific Ocean near Hawaii (station ALOHA). Deep Sea Res 40(10):2043–2060

DOE (1991) Handbook of methods for the analysis of the various parameters of the carbon dioxide system in sea water Dickson AG, Goyet C (eds). US Department of Energy

Egge JK (1993) Nutrient control of phytoplankton growth: effects of macronutrient composition (N, P, Si) on species succession. PhD thesis, University of Bergen

Goyet C, Millero FJ, Poisson A, Shafer DK (1993) Temperature dependence of CO_2 fugacity in seawater. Mar Chem 44:205–219

Goyet C, Poisson A (1989) New determination of carbonic acid dissociation constants in sea water as a function of temperature and salinity. Deep Sea Res 36(11):1635–1654

Holligan PM, Balch WM (1991) From the ocean to cells: coccolithophore optics and biogeochemistry. In: Demers S (ed) Particle analysis in oceanography. NATO ASI G27 Springer-Verlag, New York, p 301–324

Holligan PM, Fernandez E, Aiken J, Balch WM, Boyd P, Burkill PH, Finch M, Groom SB, Malin G, Muller K, Purdie DA, Robinson C, Trees CC, Turner SM, van der Wal P (1993) A biogeochemical study of the coccolithophore, *Emiliania huxleyi*, in the North Atlantic. Global Biogeochem Cycles 7(4):879–900

Mucci A (1983) The solubility of calcite and aragonite in sea water at various salinities, temperatures and one atmosphere total pressure. Am J Sci 283(7):780–799

Paasche E, Brubak S (1994) Enhanced calcification in the coccolithophorid *Emiliania huxleyi* (Haptophyceae) under phosphorus limitation. Phycologia 33:324–330

Robertson JE, Robinson C, Turner DR, Holligan P, Watson AJ, Boyd P, Fernandez E, Finch M (1994) The impact of a coccolithophore bloom on oceanic carbon uptake in the Northeast Atlantic during summer 1991. Deep Sea Res 41(2):297–314

Robertson JE, Watson AJ, Langdon C, Ling RD, Wood JW (1993) Diurnal variation in surface pCO_2 and O_2 at 60° N, 20° W in the North Atlantic. Deep Sea Res 40(1/2):409–422

Strathmann RR (1967) Estimating the organic carbon content of phytoplankton from cell volume or plasma volume. Limnol Oceanogr 12:411–418

Takahashi M, Kikuchi K, Hara Y (1985) Importance of picocyanobacteria biomass (unicellular, blue-green algae) in the phytoplankton population of the coastal waters of Japan. Mar Biol 89:63–69

Takahashi T, Olafson J, Goddard JG, Chipman DW, Sutherland SC (1990) Ratio of the organic carbon and calcium carbonate productions observed at the JGOFS 47N-20W site. JGOFS report no. 7, SCOR, Halifax

van Bleijswijk JDL, Kempers ES, van der Wal P, Westbroek P, Egge JK, Lukk T (1994a) Standing stocks of PIC, POC, PON and *Emiliania huxleyi* coccospheres and liths in sea water enclosures with different phosphate loadings. Sarsia 79:307–317

van Bleijswijk JDL, Kempers RS, Veldhuis MJ (1994b) Cell and growth characteristics of types A and B of *Emiliania huxleyi* (Prymnesiophyceae) as determined by flow cytometry and chemical analyses. J Phycol 30:230–241

van der Wal P, Kempers RS, Veldhuis MJW (1995) Production and downward flux of organic matter and calcite in a North Sea bloom of the coccolithophore *Emiliania huxleyi*. Mar Ecol Prog Ser 126:247–265

Veldhuis MJW, Kraay GW, van Bleijswijk JDL (in press) Phytoplankton biomass, productivity and growth in the western Indian Ocean during the SW- and NE-monsoons. Deep Sea Res

Wanninkhof R (1992) Relationship between wind speed and gas exchange over the ocean. J Geophys Res 97:7373–7382

Wanninkhof R, Thoning K (1993) Measurement of fugacity of CO_2 in surface water using continuous and discrete sampling methods. Mar Chem 44:189–204

Weiss RF (1974) Carbon dioxide in water and sea water: the solubility of a non-ideal gas. Mar Chem 2:203–215

Westbroek P, Brown C, van Bleijswijk J, Brownlee C, Brummer G, Conte M, Egge J, Fernández E, Jordan R, Knappertsbusch M, Stefels J, Veldhuis M, van der Wal P, Young J (1993) A model system approach to biological climate forcing. The example of *Emiliania huxleyi*. Global Planet Change 8:27–46

Westbroek P, Young JR, Linschooten K (1989) Coccolith production (biomineralization) in the marine alga *Emiliania huxleyi*. J Protozool 36(4):368–373

Young JR, Didymus JM, Mann S (1991) On the reported presence of vaterite and aragonite in coccoliths of *Emiliania huxleyi*. Botanica Mar 34:589–591

This article was submitted to the editor

Manuscript first received: November 29, 1994
Revised version accepted: July 24, 1996